Medicinal Chemistry

DOI: 10.1002/anie.201304290

Structural Analysis of Phenothiazine Derivatives as Allosteric Inhibitors of the MALT1 Paracaspase**

Florian Schlauderer, Katja Lammens, Daniel Nagel, Michelle Vincendeau, Andrea C. Eitelhuber, Steven H. L. Verhelst, Dale Kling, Al Chrusciel, Jürgen Ruland, Daniel Krappmann, and Karl-Peter Hopfner*

The human mucosa-associated lymphoid tissue lymphoma translocation protein 1 (MALT1) is responsible for the survival, proliferation, and activation of B and T lymphocytes upon antigen stimulation by means of the canonical NF-κB signaling pathway.[1] MALT1 is constitutively associated with BCL10 and assembles to form the CBM complex with CARMA1, CARMA3, or CARD9 upon activation by their individual receptors (CARMA1: CARD-containing membrane-associated guanylate kinase protein 1; CARD9: caspase-recruitment-domain-containing protein 9).[2] In the activated CBM complex MALT1 acts as a scaffolding platform and promotes the recruitment of signaling factors like tumor necrosis factor (TNF) receptor-associated factor 6 (TRAF6), transforming growth factor (TGF)-β-activated kinase (TAK1), and the regulatory subunit NEMO (NF-κB essential modulator) of the IKK complex (inhibitor of transcription factor NF-kB (IkB) kinase)[3] which finally leads to IKK activation.[4] Besides its scaffolding function, MALT1 confers proteolytic activity that is required for optimal T-cell activation.[5] Cleavage of the MALT1 substrates BCL10, A20, CYLD, and RelB results in enhanced NF-κB as well as c-Jun N-terminal kinase (JNK) activation and controls T-cell adhesion.[5a,b,6] Recent studies revealed that MALT1 is activated by ligand binding and dimerization of the paracaspase domain.[7] However, spontaneous dimerization of MALT1 in vitro leads to a catalytically inactive conformation.[7b] Hence, an additional structural rearrangement is needed for MALT1 activation that is supported by monoubiquitination in the C-terminal Ig3 domain of MALT1.[7b,8]

Modified activity of individual members of the CBM signaling complex is associated with lymphomagenesis.[9] In this context the deregulated expression of CARMA1, BCL10, and MALT1 is critical for the survival of the activated B-cell subtype of diffuse-large B-cell lymphoma (ABC-DLBCL)[10] and constitutive MALT1 paracaspase activity is a common feature of ABC-DLBCL cells. Moreover, two recent studies demonstrated the crucial role of MALT1 in the early phase of experimental autoimmune encephalomyelitis (EAE), the main animal model for multiple sclerosis (MS).[11] These results suggest that MALT1 is an important therapeutic target to treat multiple sclerosis, the most common chronic inflammatory demyelinating disease of the human central nervous system.[12] Thus, there is substantial interest in developing small-molecule compounds that specifically inhibit MALT1, a promising new approach for the treatment of MALT lymphoma, ABC-DLBCL, and multiple sclerosis.[11b,c]

Recently, distinct phenothiazines have been identified as potent small-molecule inhibitors of MALT1 that selectively kill ABC-DLBCL in vitro and in vivo.[13] The identified drugs, mepazine, thioridazine, and promazine, have a long clinical history as antipsychotics.[14] Yet, it is still unclear how these substances inhibit MALT1. A detailed understanding of the binding mode is crucial to further optimize the efficacy and selectivity of these compounds for clinical use.

Here, we report the crystal structure of ligand-free dimeric human $MALT1_{Casp\text{-}Ig3}$ in complex with the tricyclic phenothiazine derivative thioridazine. Unexpectedly, the structure reveals that the inhibitor binds in a pocket located opposite to the caspase active site, in the interface between

[*] F. Schlauderer,[+] Dr. K. Lammens,[+] Prof. K.-P. Hopfner
Gene Center, Department of Biochemistry
Ludwig-Maximilians University Munich
Feodor-Lynen-Strasse 25, 80377 Munich (Germany)
E-mail: klammens@genzentrum.lmu.de
D. Nagel, Dr. M. Vincendeau, Dr. A. C. Eitelhuber, Dr. D. Krappmann
Research Unit Cellular Signal Integration
Institute of Molecular Toxicology and Pharmacology
Helmholtz Zentrum München
Ingolstädter Landstrasse 1, 85764 Neuherberg (Germany)
Dr. S. H. L. Verhelst
Lehrstuhl für Chemie der Biopolymere
Technische Universität München
Weihenstephaner Berg 3, 85354 Freising (Germany)
D. Kling, A. Chrusciel
Kalexsyn, Inc.
4502 Campus Drive, Kalamazoo, MI 49008 (USA)
Prof. Dr. J. Ruland
Institut für Klinische Chemie und Pathobiochemie
Klinikum rechts der Isar, Technische Universität München
81675 München (Germany)
[+] These authors contributed equally to this work.

[**] We thank C. Basquin for the CD measurements and G. Witte for help with the fluorescence quenching assays. We thank the Max-Planck Crystallization Screening Facility for initial crystallization trials. We thank the Swiss Light Source (SLS, Villigen, Switzerland) and the European Synchrotron Radiation Facility (ESRF, Grenoble, France) for beam time and onsite support. S.V. is supported by the DFG (Emmy Noether program); F.S., K.L., D.K., and K.P.H. are supported by the SFB 1054.

Supporting information for this article is available on the WWW under http://dx.doi.org/10.1002/anie.201304290.

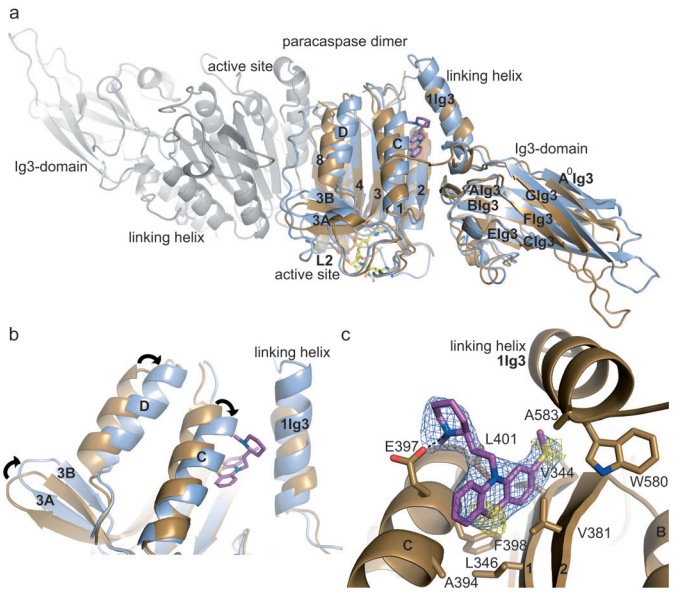

Figure 1. Thioridazine binds at an allosteric position in the interface between the paracaspase and Ig3 domain connecting helix α1Ig3.[17] a) Superposition of MALT1$_{Casp\text{-}Ig3}$ bound to hex-LRSR-peptide (light blue) and in complex with thioridazine (gold). The biologically relevant MALT1 dimer is shown in gray. b) The conformational rearrangement of helix αC and αD and subsequently β-sheets 3A and 3B is inhibited due to the steric hindrance by thioridazine. c) Close-up view of the hydrophobic binding pocket; the residues that interact with thioridazine are shown as sticks. The violet mesh represents the refined $2F_o-F_c$ electron density map (contoured at 1 σ) for the ligand, shown together with the anomalous difference density map (contoured at 2.2 σ and shown in yellow).

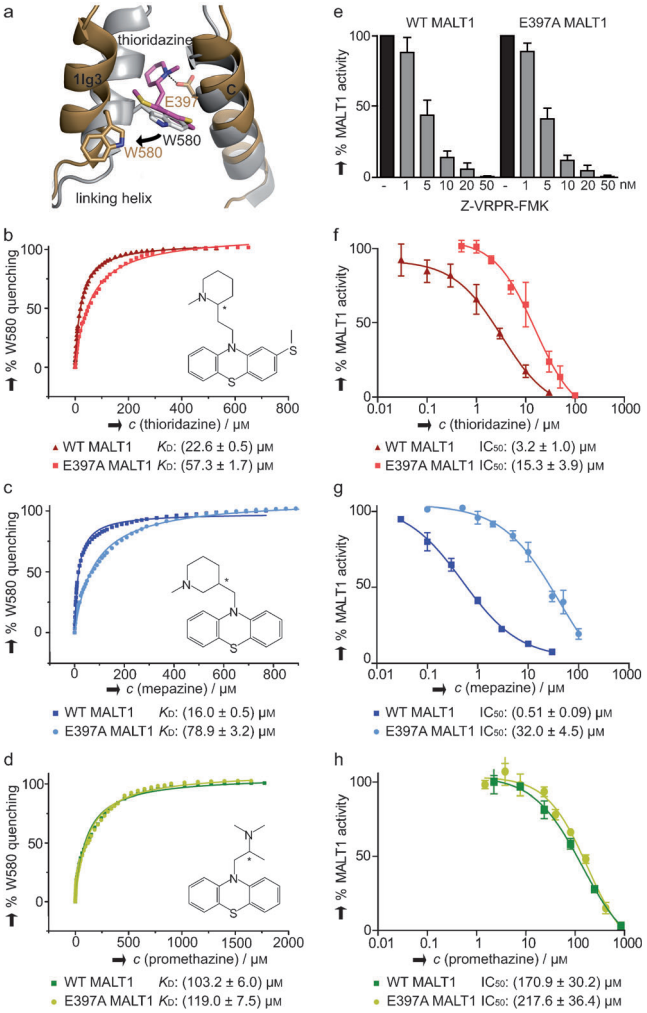

Figure 2. MALT1 mutant E397A is less responsive to the inhibitory potential of mepazine and thioridazine. a) Close up view of W580 flipping and the interaction of thioridazine with residue E397. The thioridazine-bound and ligand-free MALT1 structures are shown in gold and gray, respectively (PDB code: 3V55).[7b] b–d) Tryptophan fluorescence quenching titration study of monomeric MALT1$_{Casp\text{-}Ig3}$ and the E397A mutant with thioridazine, mepazine, and promethazine (negative control). The binding constants of the different phenothiazine inhibitors to the wt and mutant protein are listed below the respective graphs. e) Activity of MALT1 wt and E397A is inhibited by the peptide-based MALT1 inhibitor Z-VRPR-FMK. Increasing amounts of the peptide led to an equivalent loss of MALT1 activity. The data confirmed that the mutant E397A has no influence on the activity of MALT1. f–h) MALT1 cleavage assay performed with wt and E397A GST-MALT1$_{325\text{-}760}$ after incubation with mepazine, thioridazine, and promethazine. Mepazine and thioridazine have a lower inhibitory potential on the E397A mutant than on the wt, while the impact of the weak MALT1 inhibitor promethazine on both MALT1 variants is equivalent.

the caspase domain and the Ig3 domain connecting helix α1$_{Ig3}$ of MALT1 (Figure 1 a). This allosteric binding site, far from the catalytic center well explains the fact that phenothiazine derivatives act as noncompetitive, reversible inhibitors.[13] Superposition of the enzymatic active MALT1$_{Casp\text{-}Ig3}$ construct bound to the hex-LRSR-AOMK peptide (unpublished data) with the thioridazine-bound structure indicate, that binding of the compound between helices α1$_{Ig3}$ and αC prevents the conformational change into an active enzyme, the so-called second activation step of MALT1[7b] (Figure 1). Besides ligand-induced rearrangements of the active site loops three major shifts of helices αC, αD, and of β-sheets 3A and 3B are essential to achieve the enzymatic proficient protease conformation (Figure 1 b). The movement of helices αC and αD is hampered by the sandwiched thioridazine, and subsequently β-sheets 3A and 3B cannot perform their pivotal shift (Figure 1 b). A detailed analysis of the inhibitor binding site shows that the tricyclic ring system of thioridazine is bound in a hydrophobic pocket composed of residues A394, F398, and L401 in helix αC and L346, V344, and V381 in β-sheets 1 and 2, respectively (Figure 1 c). The orientation of the 2-methylthiophenothiazine ring was proven by collecting a dataset at a wavelength of 1.9 Å to detect the anomalous signal of sulfur (Figure 1 c).

Upon inhibitor binding, the side chain of residue tryptophan W580 on helix α1$_{Ig3}$ is flipped out of the hydrophobic groove into a solvent-exposed environment which leads to a substantial displacement of helix α1$_{Ig3}$ (Figure 2 a). Probably triggered by rotation of this domain-connecting helix, the entire Ig3 domain becomes more flexible (Figure 1 a). To verify the mechanism of inhibition by phenothiazine-based drugs with MALT1 in solution, we developed a tryptophan-fluorescence-quenching assay. For this assay we took advantage of the fact that W580 is the only tryptophan residue in the MALT1$_{Casp\text{-}Ig3}$ construct and in close proximity to the bound tricyclic compound. The tryptophan fluorescence of mono-

meric $MALT1_{Casp\text{-}Ig3}$ was recorded with increasing amounts of thioridazine (Figure 2b). The titration was continued until saturation of quenching was observed.

To confirm that the titration of thioridazine has no effect on the general folding of $MALT1_{Casp\text{-}Ig3}$ under the applied conditions, circular dichroism spectra were collected (Figure 1 in the Supporting Information). The association constants were calculated by plotting the percentage of W580 quenching versus the concentration of the compound and fitting the curves to a one-site binding model. The equivalent experiment was conducted using mepazine; similar results led to the proposal that different phenothiazine derivatives inhibit MALT1 by the same mechanism (Figure 2c). As a negative control, the weak inhibitory phenothiazine-based compound promethazine was used in the tryptophan-quenching assay (Figure 2d); promethazine showed a significant lower binding constant, consistent with the weak inhibitory effect in vivo.[13]

The structure of inhibitor-bound MALT1 well explains the effect of different phenothiazine modifications on their inhibitory effectiveness as Nagel et al. had described. On the one hand, the phenothiazine ring system has an optimal size to fit in the hydrophobic pocket and only minor changes that increase the size or enhance the solubility are tolerated. On the other hand, the hydrogen bond between the *N*-methylpiperidine nitrogen of thioridazine and glutamic acid E397 seems to play a major role in MALT1 recognition (Figure 2a), as the phenothiazine backbone alone is a very weak MALT1 inhibitor. All derivatives tested with a piperidyl ring system and/or nitrogen in a similar position to the piperidyl nitrogen showed an inhibitory effect in comparable range.[13] Modifications in the connecting alkyl chain, for example keto- or hydroxy groups, increased the IC_{50} values up to tenfold.[13] We concluded that the tricyclic ring system and the methylpiperidyl group play equally important roles in drug recognition. To verify the influence of the E397–thioridazine interaction and to further support the proposed binding mechanism for phenothiazine derivatives, an E397A mutant of MALT1 was tested with regard to its inhibition by different phenothiazine derivatives in vitro and in vivo. To ensure correct folding of the mutant protein, an in vitro enzymatic activity assay was performed (Figure 2e). To define the inhibitory potential on wild-type (wt) and mutant MALT1, IC_{50} values were determined for thioridazine, mepazine, and promethazine on GST-$MALT1_{325\text{-}760}$ wt and E397A (Figure 2f–h). The two compounds with a piperidyl ring system, thioridazine and mepazine, display a lower inhibitory potential on the E397A mutant than on the wt, whereas the mutation had no influence on the weak inhibitory effect of promethazine. These results are consistent with the tryptophan-quenching data and emphasize the importance of the E397–inhibitor interaction on the inhibitory potential of these phenothiazine derivatives in vitro.

To test the proposed inhibitor-binding mechanism in cells, the human cell line HBL-1 derived from DLBCL patients was transduced with wildtype or E397A mutant MALT1. After doxycycline-induced MALT1 expression the cells were exposed to either mepazine or thioridazine. Analysis of cell viability by cell count four days after treatment revealed that both compounds reduced the viability of cells transduced with MALT1 wildtype, while the HBL-1 cells transduced with the E397A mutant were largely resistant to mepazine and thioridazine (Figure 3). FACS histograms and western blot show that MALT wildtype and E397A mutant proteins are only expressed after addition of doxycycline (Figure 2a,b in the Supporting Information).

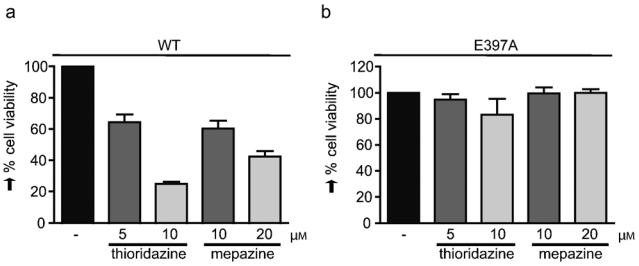

Figure 3. HBL-1 cells were lentivirally transduced with either MALT1 wildtype or the point mutant E397A. Subsequently, they were treated with mepazine and thioridazine, and cell viability was monitored after four days. The data demonstrate that mepazine and thioridazine diminish cell viability of cells expressing MALT1 wt, while the E397A mutant confers increased resistance to the compounds.

A detailed inspection of the electron density map of the inhibitor suggests that solely the *S* enantiomer of thioridazine is bound in the crystal structure (Figure 1c). However, we cannot exclude that the *R* enantiomer is able to bind with comparable affinity at this position. To analyze the influence of chirality on the binding affinity and inhibitory potential of the individual enantiomers, (*R*)- and (*S*)-mepazine and thioridazine were prepared in enantiomerically pur form pure as described in the Supporting Information and analyzed accordingly. Whereas (*R*)- and (*S*)-thioridazine show equivalent binding affinities and IC_{50} values (Figure 4a,c) (*S*)-mepazine exhibits a significantly higher binding affinity and an up to eight times higher inhibitory potential over (*R*)-mepazine (Figure 4b,d). So far thioridazine has been applied in the racemic form as the hydrochloride of 10-[2-(1-methylpiperid-2-yl)ethyl]-2-methylthiophenothiazine for the symptomatic therapy of psychotic disorders.[14] Nevertheless, the antipsychotic effect is believed to be associated with (*R*)-thioridazine.[15] Since (*S*)-thioridazine binds MALT1 with a comparable affinity, it may be possible to reduce the sedative effects by using the pure *S* enantiomer for treatment of MALT1-driven cancer or autoimmune diseases. In any case, the increased affinity of (*S*)-mepazine represents the first step towards an MALT1-optimized phenothiazine-based compound.

Since the 1950s thioridazine, mepazine, and other phenothiazines have been used clinically as antipsychotic drugs, where they exert their sedative effects by acting as dopamine receptor antagonists in the brain.[14] Recently, thioridazine was shown to induce toxicity in cancer stem cells (CSCs) while having no effect on normal human pluripotent stem cells (hPSCs). However, quite in contrast to the situation found in MALT1-dependent ABC-DLBCL, CSCs express dopamine receptors, and thioridazine affects CSC survival by acting as

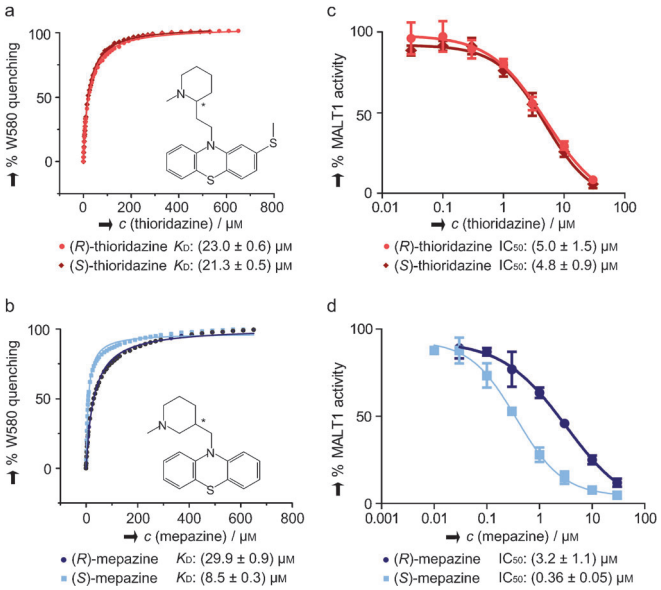

Figure 4. Mepazine enantiomers have different MALT1 inhibitory potentials. a,b) Tryptophan-quenching assay with the separated *R* and *S* enantiomers of thioridazine and mepazine. c,d) MALT1 cleavage assay with wt GST-MALT1$_{325\text{-}760}$ after incubation with either the *R* or *S* enantiomer of mepazine and thioridazine. c) Thioridazine enantiomers have an equivalent MALT1 inhibitory potential. d) (*S*)-mepazine has a higher MALT1 inhibitory potential than the *R* enantiomer.

a dopamine receptor antagonist.[16] Whereas side effects associated with dopamine receptors may be tolerated to some extent for treatment of high-grade MALT1-dependent lymphoma, more selective MALT1 inhibitors are certainly required for a therapeutic application in diseases associated with autoimmunity or allergic inflammation. By identifying the thioridazine and mepazine binding pocket on the new target MALT1, we pave the way for medicinal chemistry to develop effective MALT1 inhibitors. From the perspective of structure-based drug design, the detailed analysis of the key binding interactions in the co-crystal structure provides important insights for further optimization of a phenothiazine-based MALT1 inhibitor. The identification of the improved affinity of (*S*)-mepazine represents a significant result towards this goal. Thus, our structural insights into the noncompetitive, allosteric mode of MALT1 inhibition will be of significance for the development of more effective and selective drugs to treat MALT1-driven cancer or autoimmune diseases.

Received: May 18, 2013
Published online: August 14, 2013

Keywords: cancer · inhibitors · medicinal chemistry · multiple sclerosis · thioridazine

[1] M. Thome, *Nat. Rev. Immunol.* **2008**, *8*, 495 – 500.
[2] a) A. G. Uren, K. O'Rourke, L. A. Aravind, M. T. Pisabarro, S. Seshagiri, E. V. Koonin, V. M. Dixit, *Mol. Cell* **2000**, *6*, 961 – 967; b) H. Zhou, M. Q. Du, V. M. Dixit, *Cancer Cell* **2005**, *7*, 425 – 431.
[3] a) L. Sun, L. Deng, C. K. Ea, Z. P. Xia, Z. J. Chen, *Mol. Cell* **2004**, *14*, 289 – 301; b) O. Gaide, B. Favier, D. F. Legler, D. Bonnet, B. Brissoni, S. Valitutti, C. Bron, J. Tschopp, M. Thome, *Nat. Immunol.* **2002**, *3*, 836 – 843.
[4] A. Oeckinghaus, E. Wegener, V. Welteke, U. Ferch, S. C. Arslan, J. Ruland, C. Scheidereit, D. Krappmann, *EMBO J.* **2007**, *26*, 4634 – 4645.
[5] a) F. Rebeaud, S. Hailfinger, A. Posevitz-Fejfar, M. Tapernoux, R. Moser, D. Rueda, O. Gaide, M. Guzzardi, E. M. Iancu, N. Rufer, N. Fasel, M. Thome, *Nat. Immunol.* **2008**, *9*, 272 – 281; b) B. Coornaert, M. Baens, K. Heyninck, T. Bekaert, M. Haegman, J. Staal, L. Sun, Z. J. Chen, P. Marynen, R. Beyaert, *Nat. Immunol.* **2008**, *9*, 263 – 271; c) M. Duwel, V. Welteke, A. Oeckinghaus, M. Baens, B. Kloo, U. Ferch, B. G. Darnay, J. Ruland, P. Marynen, D. Krappmann, *J. Immunol.* **2009**, *182*, 7718 – 7728.
[6] a) S. Hailfinger, H. Nogai, C. Pelzer, M. Jaworski, K. Cabalzar, J. E. Charton, M. Guzzardi, C. Decaillet, M. Grau, B. Dorken, P. Lenz, G. Lenz, M. Thome, *Proc. Natl. Acad. Sci. USA* **2011**, *108*, 14596 – 14601; b) S. Rosebeck, P. C. Lucas, L. M. McAllister-Lucas, *Future Oncol.* **2011**, *7*, 613 – 617; c) J. Staal, Y. Driege, T. Bekaert, A. Demeyer, D. Muyllaert, P. Van Damme, K. Gevaert, R. Beyaert, *EMBO J.* **2011**, *30*, 1742 – 1752.
[7] a) J. Hachmann, S. J. Snipas, B. J. van Raam, E. M. Cancino, E. J. Houlihan, M. Poreba, P. Kasperkiewicz, M. Drag, G. S. Salvesen, *Biochem. J.* **2012**, *443*, 287 – 295; b) C. Wiesmann, L. Leder, J. Blank, A. Bernardi, S. Melkko, A. Decock, A. D'Arcy, F. Villard, P. Erbel, N. Hughes, F. Freuler, R. Nikolay, J. Alves, F. Bornancin, M. Renatus, *J. Mol. Biol.* **2012**, *419*, 4 – 21; c) J. W. Yu, P. D. Jeffrey, J. Y. Ha, X. Yang, Y. Shi, *Proc. Natl. Acad. Sci. USA* **2011**, *108*, 21004 – 21009.
[8] C. Pelzer, K. Cabalzar, A. Wolf, M. Gonzalez, G. Lenz, M. Thome, *Nat. Immunol.* **2013**, *14*, 337 – 345.
[9] L. M. Staudt, *Cold Spring Harbor Perspect. Biol.* **2010**, *2*, a000109.
[10] V. N. Ngo, R. E. Davis, L. Lamy, X. Yu, H. Zhao, G. Lenz, L. T. Lam, S. Dave, L. Yang, J. Powell, L. M. Staudt, *Nature* **2006**, *441*, 106 – 110.
[11] a) A. G. Baxter, *Nat. Rev. Immunol.* **2007**, *7*, 904 – 912; b) C. Mc Guire, P. Wieghofer, L. Elton, D. Muylaert, M. Prinz, R. Beyaert, G. van Loo, *J. Immunol.* **2013**, *190*, 2896 – 2903; c) A. Brüstle, D. Brenner, C. B. Knobbe, P. A. Lang, C. Virtanen, B. M. Hershenfield, C. Reardon, S. M. Lacher, J. Ruland, P. S. Ohashi, T. W. Mak, *J. Clin. Invest.* **2012**, *122*, 4698 – 4709.
[12] B. D. Trapp, K. A. Nave, *Annu. Rev. Neurosci.* **2008**, *31*, 247 – 269.
[13] D. Nagel, S. Spranger, M. Vincendeau, M. Grau, S. Raffegerst, B. Kloo, D. Hlahla, M. Neuenschwander, J. P. von Kries, K. Hadian, B. Dorken, P. Lenz, G. Lenz, D. J. Schendel, D. Krappmann, *Cancer Cell* **2012**, *22*, 825 – 837.
[14] P. Seeman, T. Lee, *Science* **1975**, *188*, 1217 – 1219.
[15] S. A. Jortani, A. Poklis, *J. Anal. Toxicol.* **1993**, *17*, 374 – 377.
[16] E. Sachlos, R. M. Risueno, S. Laronde, Z. Shapovalova, J. H. Lee, J. Russell, M. Malig, J. D. McNicol, A. Fiebig-Comyn, M. Graham, M. Levadoux-Martin, J. B. Lee, A. O. Giacomelli, J. A. Hassell, D. Fischer-Russell, M. R. Trus, R. Foley, B. Leber, A. Xenocostas, E. D. Brown, T. J. Collins, M. Bhatia, *Cell* **2012**, *149*, 1284 – 1297.
[17] The structure of MALT1$_{Casp\text{-}Ig3}$ in complex with thioridazine is deposited in the Protein Data Base under accession code 4I1R.

